1N

NATIONAL AERONAUTICS AND SPACE ADMINISTRATION

TECHNICAL MEMORANDUM X-134

SIDESLIP CHARACTERISTICS AT VARIOUS ANGLES OF ATTACK FOR SEVERAL HYPERSONIC MISSILE CONFIGURATIONS WITH CANARD CONTROLS AT A MACH NUMBER OF 2.01*

By Gerald V. Foster

SUMMARY

An investigation has been made in the Langley 4- by 4-foot supersonic pressure tunnel to determine the aerodynamic characteristics at a Mach number of 2.01 of a series of hypersonic missile configurations. The configurations investigated included a body of revolution having a length-diameter ratio of 10, a body with a 10° flare at the base, and a body with cruciform fins of 5° or 15° apex angle at the base. The configurations with fins and flare were equipped with canard surfaces for pitch control.

The results indicated large variations in normal force and pitching moment with sideslip angle due to canard-control deflection for both the finned and flared configurations; however, this effect diminished as the angle of attack increased. The canard controls, however, had little effect on the rolling-moment characteristics of the flared configuration; whereas, substantial induced roll was indicated for the finned configurations.

INTRODUCTION

An investigation has been conducted in the Langley 4- by 4-foot supersonic pressure tunnel to study the stability and control characteristics at a Mach number of 2.01 of a series of missile configurations. This series included four models consisting basically of a body of revolution having a length-diameter ratio of 10. The configurations investigated other than the basic configuration included a body with a 10° flare at the base, a body with 5° cruciform fins, and a body with 15° cruciform fins.

*Title, Unclassified.

The purpose of this investigation was to determine the effects of afterbody-flare and cruciform-fin arrangements on the longitudinal and lateral aerodynamic characteristics of a body of revolution. In addition, the effects of canard surfaces on the aerodynamic characteristics of the flared-afterbody and cruciform-fin configurations were investigated. Data pertaining to the longitudinal stability and control characteristics of these configurations as well as lateral stability characteristics for small angles of sideslip are presented in reference 1.

The purpose of the present paper is to supplement reference 1 by providing aerodynamic data for these missile configurations at combined angles of attack and sideslip up to approximately 24°.

COEFFICIENTS AND SYMBOLS

The results presented herein are referred to the body-axis system (fig. 1). The moment reference point is at a longitudinal station corresponding to the 50-percent-body station.

The coefficients and symbols are defined as follows:

C_N normal-force coefficient, F_N/qS

C_m pitching-moment coefficient, M_Y/qSd

C_l rolling-moment coefficient, M_X/qSd

C_n yawing-moment coefficient, M_Z/qSd

C_Y side-force coefficient, F_Y/qS

F_N normal force

F_Y side force

M_Y pitching moment, moment about Y-axis

M_X rolling moment, moment about X-axis

M_Z yawing moment, moment about Z-axis

q	free-stream dynamic pressure
d	diameter of cylindrical section of body
S	cross-sectional area of cylindrical section of body
R	radius
C	canard surface (horizontal only) subscripts 1, 2, 3 (see fig. 3)
M	Mach number
α	angle of attack, deg
β	angle of sideslip, deg
δ_c	angle of canard deflection, positive for trailing edge down, deg

MODEL AND APPARATUS

Details of the various complete model configurations are shown in figure 2, and details of the canard controls C_1, C_2, C_3 are shown in figure 3. Geometric characteristics of the model are given in table I. Photographs of the model with 10° flare and 5° fins are presented in figure 4.

The basic body configuration consisted of an ogive forebody with a rounded nose having a straight taper to accommodate the canard controls. The cylindrical body section housed a six-component strain-gage balance. Coordinates for the forebody of the basic body are given in reference 1. The other body configurations were obtained by attaching either a flare or cruciform fins to the cylindrical section of the basic body. The fins and canard surfaces consisted of flat plates with round leading edges. The fins had blunt trailing edges; whereas the canard surfaces had round trailing edges. The canard surfaces were located in the horizontal plane with the hinge line located approximately 9 percent back of the forebody apex.

The models were mounted on a rotary sting to permit testing through ranges of combined angles of attack and sideslip.

TESTS, CORRECTIONS, AND ACCURACY

The test conditions are as follows:

Mach number	2.01
Stagnation temperature, °F	100
Stagnation pressure, lb/sq in. abs	8.05
Reynolds number, per ft	2×10^6

The stagnation dewpoint was maintained sufficiently low (-25° F or less) so that no condensation effects were encountered in the test section.

Tests were made through a sideslip range from 0° to a maximum of about 24° at angles of attack of approximately 0°, 12°, and 24°.

The angles of attack and sideslip were corrected for the deflection of the balance and sting under load.

The estimated accuracy of the individual measured quantities is as follows:

C_N	±0.034
C_m	±0.099
C_l	±0.005
C_n	±0.099
C_Y	±0.032
α, deg	±0.1
β, deg	±0.1
δ_c, deg	±0.1
M	±0.015

DISCUSSION

Effects of Fin Plan Form and Afterbody Flare

The aerodynamic characteristics of the various body configurations investigated through a range of sideslip angles are presented in figure 5. In general, these results indicate that the addition of either 15° fins or a 10° flare resulted in changes in C_N and C_m which were approximately constant with sideslip angle up to a moderately large value of β (approximately 16°). As a consequence the longitudinal stability characteristics of either the 15° fin configuration or the 10° flare configuration reported in reference 1, would not be significantly different for a condition of sideslip up to moderatly large values. It may be noted that this is also true for 5° fins up to a sideslip angle of approximately 8°; however, at sideslip angles greater than 8° the C_N and C_m obtained with 5° fins decreased significantly.

Effect of Canard Surface

The effects of canard controls on the aerodynamic characteristics of the various body configurations in sideslip are presented in figures 6 to 8. The addition of canard controls ($\delta_c = 0^{\circ}$) had no significant effect on the aerodynamic characteristics at $\alpha = 0^{\circ}$, whereas deflected canard controls appeared to have altered the loading characteristics over the rear part of the body, resulting in changes in both the longitudinal and lateral aerodynamic characteristics of the various configurations in sideslip (figs. 6 to 8). For example, the results obtained with either the flared or finned configuration at $\alpha = 0^{\circ}$ indicate that with canard controls deflected there was a gradual increase in C_N with increase in β up to moderate values of β, accompanied by a decrease in positive C_m. However, with further increase in β, C_N decreased and C_m increased in a positive direction (figs. 6 to 8). Canard-control deflection also resulted in nonlinear variations of C_l with β for the finned configurations (figs. 7 to 8) but had little effect on C_l for the flared configuration (fig. 6). On the basis of results presented in reference 2, it would appear that the changes in C_N and C_m are associated with the effects of canard-control vorticity on both the horizontal fins and the afterbody, whereas the changes in C_l appear to result from canard-control-induced effects on both the vertical and the horizontal fins. It may be noted by comparison of the rolling-moment results obtained with a 5° fin configuration (fig. 8) that the induced roll due to the long-chord canard control C_2 was maintained to a slightly larger angle of attack than for either of the shorter chord canard controls C_1 and C_3. This is attributed partially to the location of the source of canard-control vorticity being nearer to the fins with the longer chord canard controls.

SUMMARY OF RESULTS

An investigation was made of the effects of fins and afterbody flare on a missile configuration having a length-diameter ratio of 10. The results indicate that variation in sideslip angle had no significant effect on the longitudinal stability with 15° fins or 10° flared afterbody up to moderately large values of sideslip (approximately 16°) or to approximately 8° sideslip angle with the 5° fins. Deflecting the canard surfaces, resulted in large variation in normal-force and pitching-moment increment for configurations with either fins or flared afterbody through the range of sideslip angles; however, this effect diminished as the angle of attack increased. The canard surfaces, however, had little effect on the rolling moments of the flared configuration, whereas substantial induced rolling moments were indicated for the finned configurations.

I
2
6
2

Langley Research Center,
National Aeronautics and Space Administration,
Langley Field, Va., August 3, 1959.

REFERENCES

1. Robinson, Ross B.: Wind-Tunnel Investigation at a Mach Number of 2.01 of the Aerodynamic Characteristics in Combined Angles of Attack and Sideslip of Several Hypersonic Missile Configurations With Various Canard Controls. NACA RM L58A21, 1958.

2. Robinson, Ross B., and Spearman, M. Leroy: Aerodynamic Characteristics for Combined Angles of Attack and Sideslip of a Low-Aspect-Ratio Cruciform-Wing Missile Configuration Employing Various Canard and Trailing-Edge Flap Controls at a Mach Number of 2.01. NASA MEMO 10-2-58L, 1958.

TABLE I.- MODEL DIMENSIONS

Body:	
Length, in.	30.00
Diameter, in.	3.00
Cross-sectional area, sq in.	7.07
Fineness ratio of nose	5.00
Length-diameter ratio	10.00
Moment center location, percent length	50.0
10° flare:	
Length, in.	6.01
Base diameter, in.	5.13
Base area, sq in.	20.66

	5° fins	15° fins
Fins:		
Area, exposed, 2 fins, sq in.	34.36	9.55
Root chord, in.	19.12	5.97
Tip chord, in.	0	0
Span, exposed, 2 fins, in.	3.20	3.20
Span, total, 2 fins, in.	6.20	6.20
Taper ratio	0	0
Aspect ratio, exposed	0.268	0.075
Span diameter ratio	2.07	2.07
Leading-edge sweep, deg	85	75

	C_1	C_2	C_3
Canard surfaces:			
Area, exposed, sq in.	5.20	7.76	7.88
Span, total, in.	3.00	3.00	4.86
Leading-edge sweep angle, deg	45.0	45.0	45.0
Area ratio (to 5° fins)	0.15	0.23	0.23
Area ratio (to 15° fins)	0.54	0.81	0.82

[redacted]

L-262

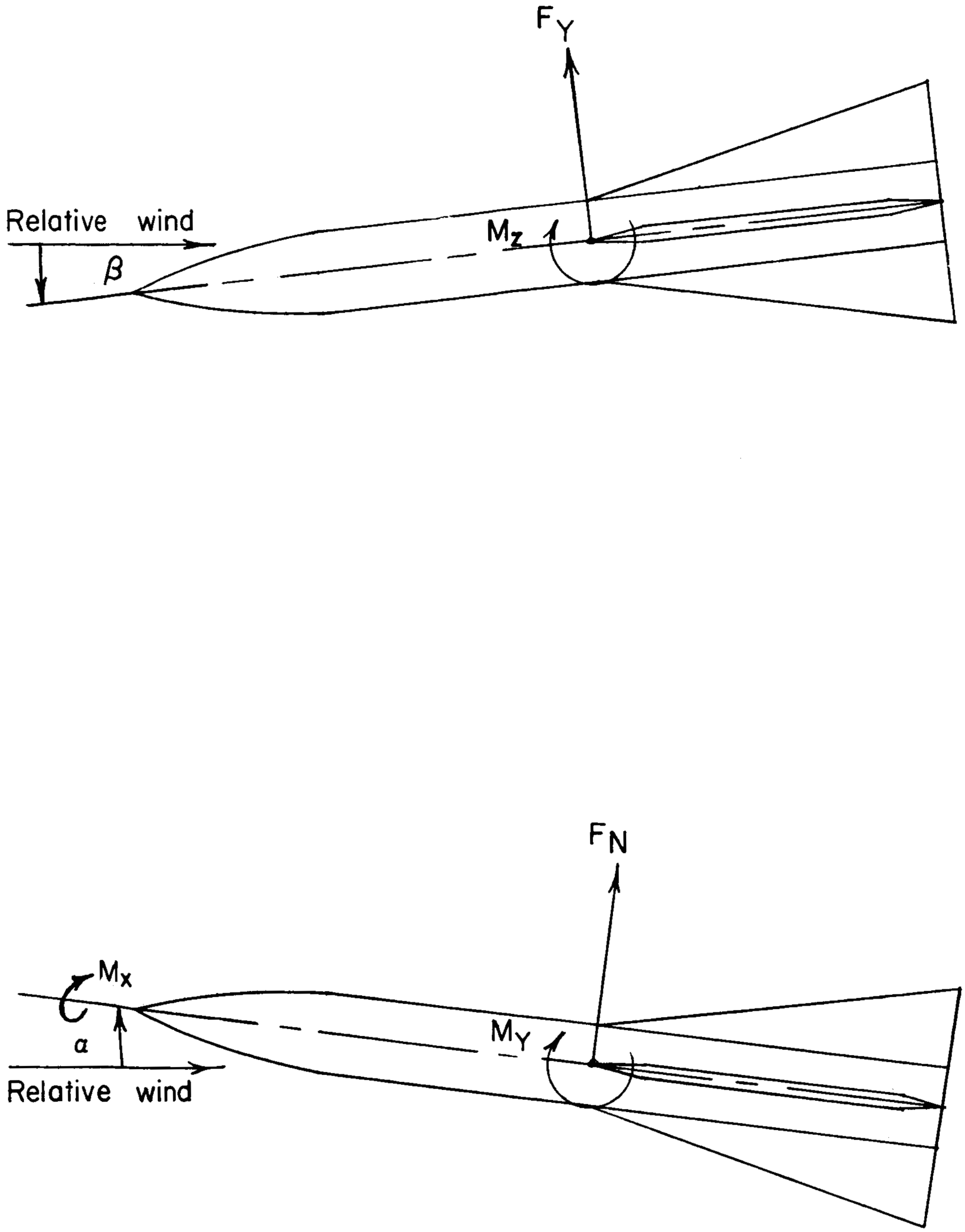

Figure 1.- Body-axis system. Arrows indicate positive directions of forces, moments, and angles.

[redacted]

L-262

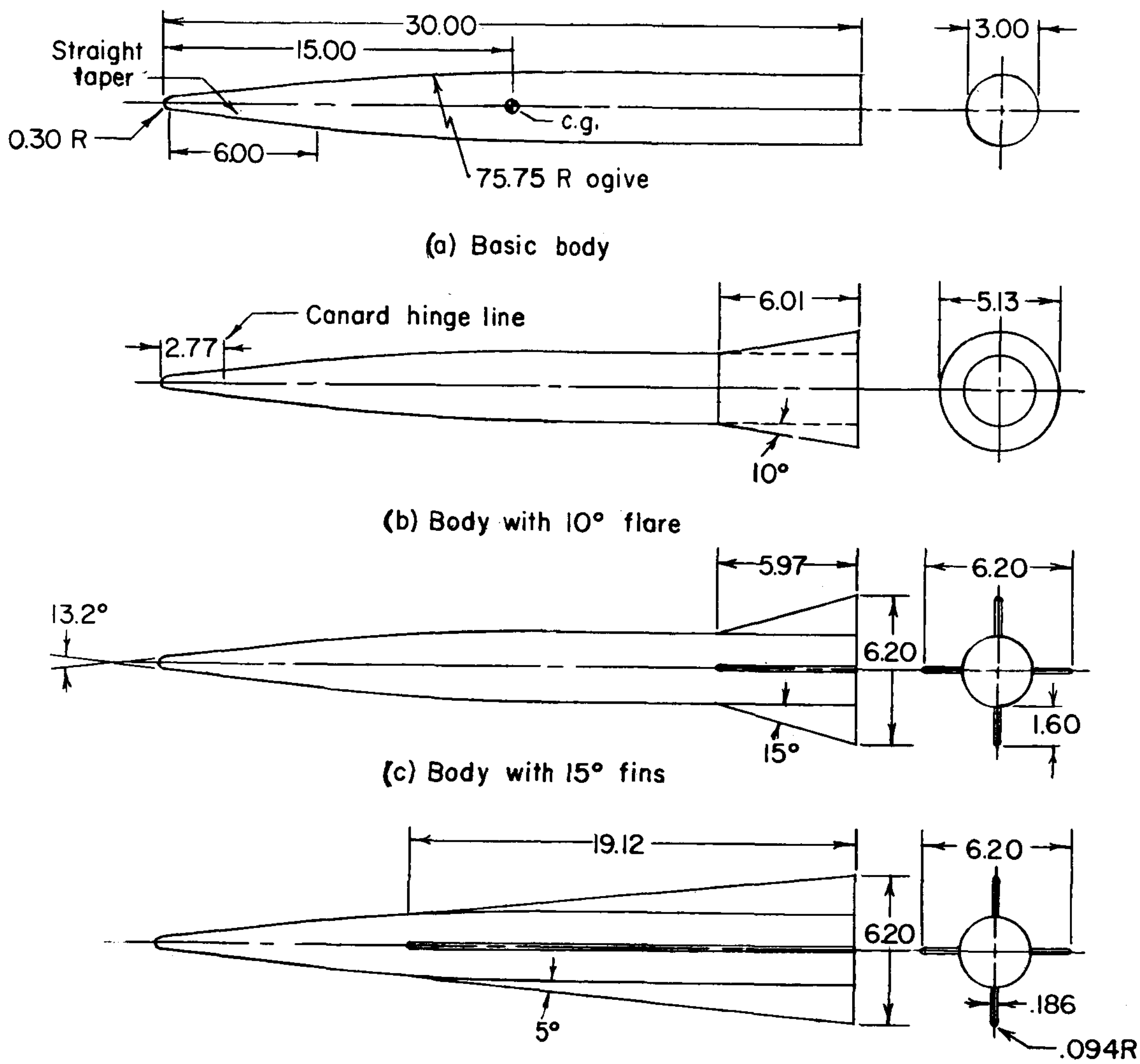

Figure 2.- Sketches of complete models. Linear dimensions are in inches.

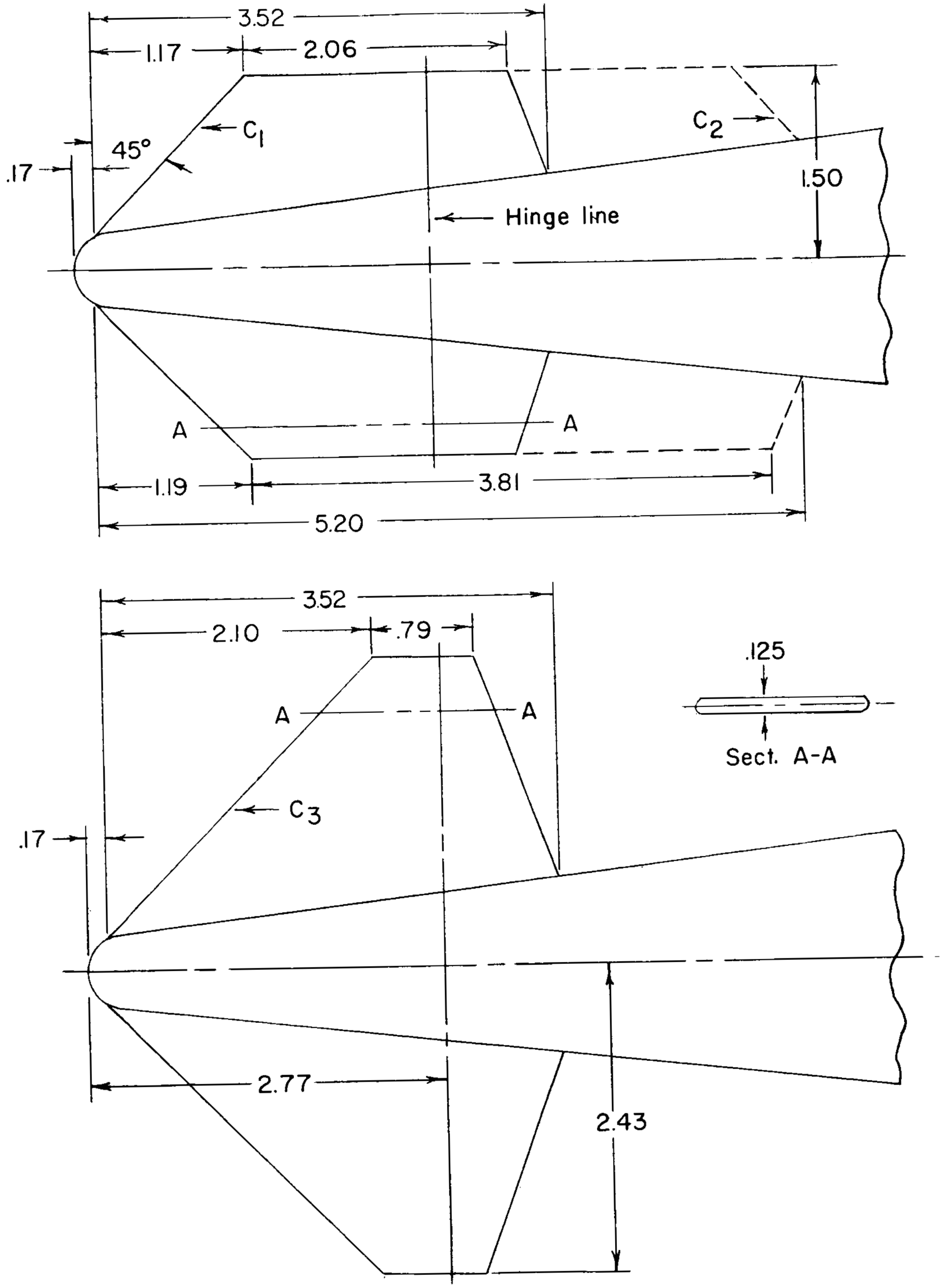

Figure 3.- Details of canard controls. Linear dimensions are in inches.

[redacted]

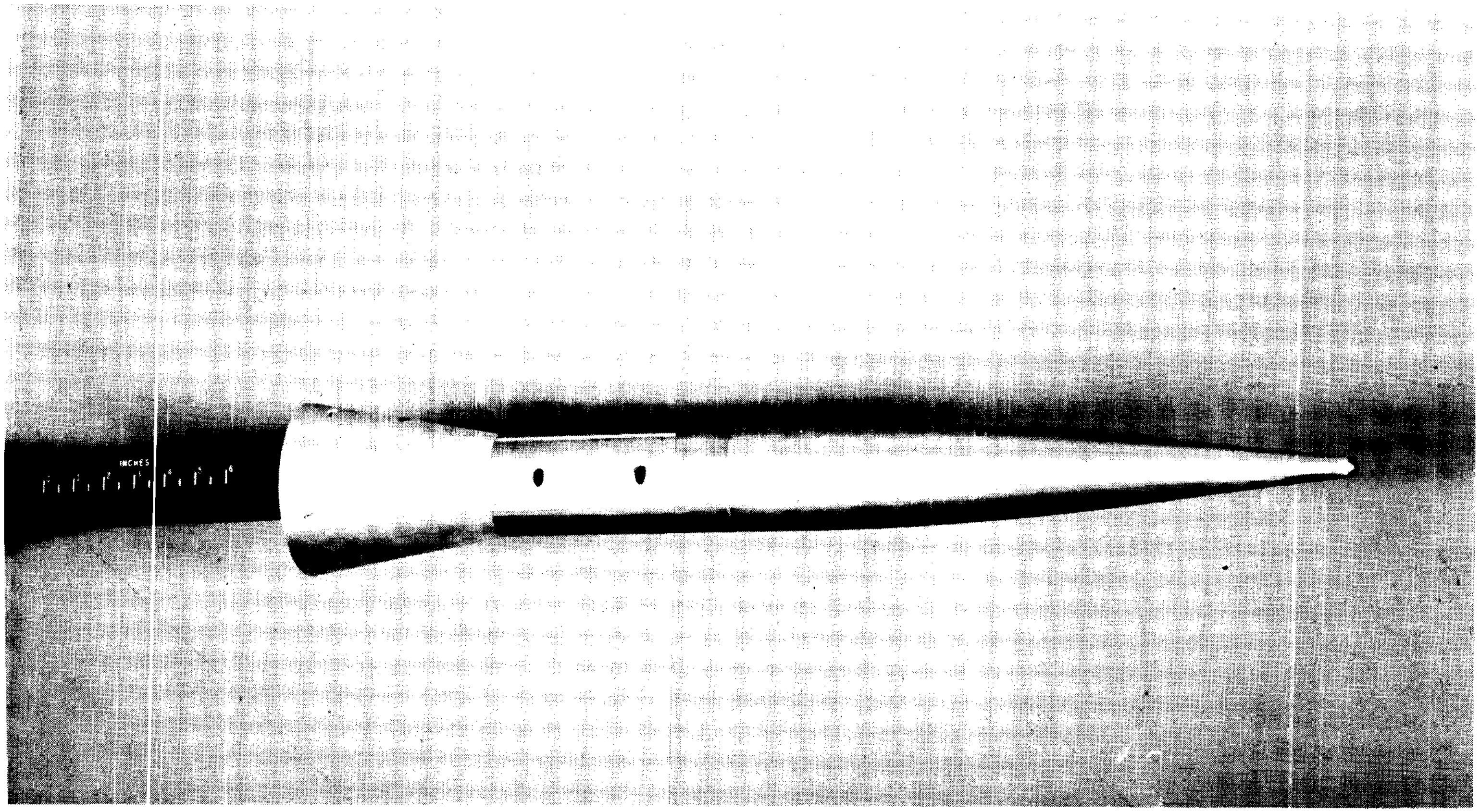

(a) Body with flared afterbody. L-57-2412

Figure 4.- Photographs of models.

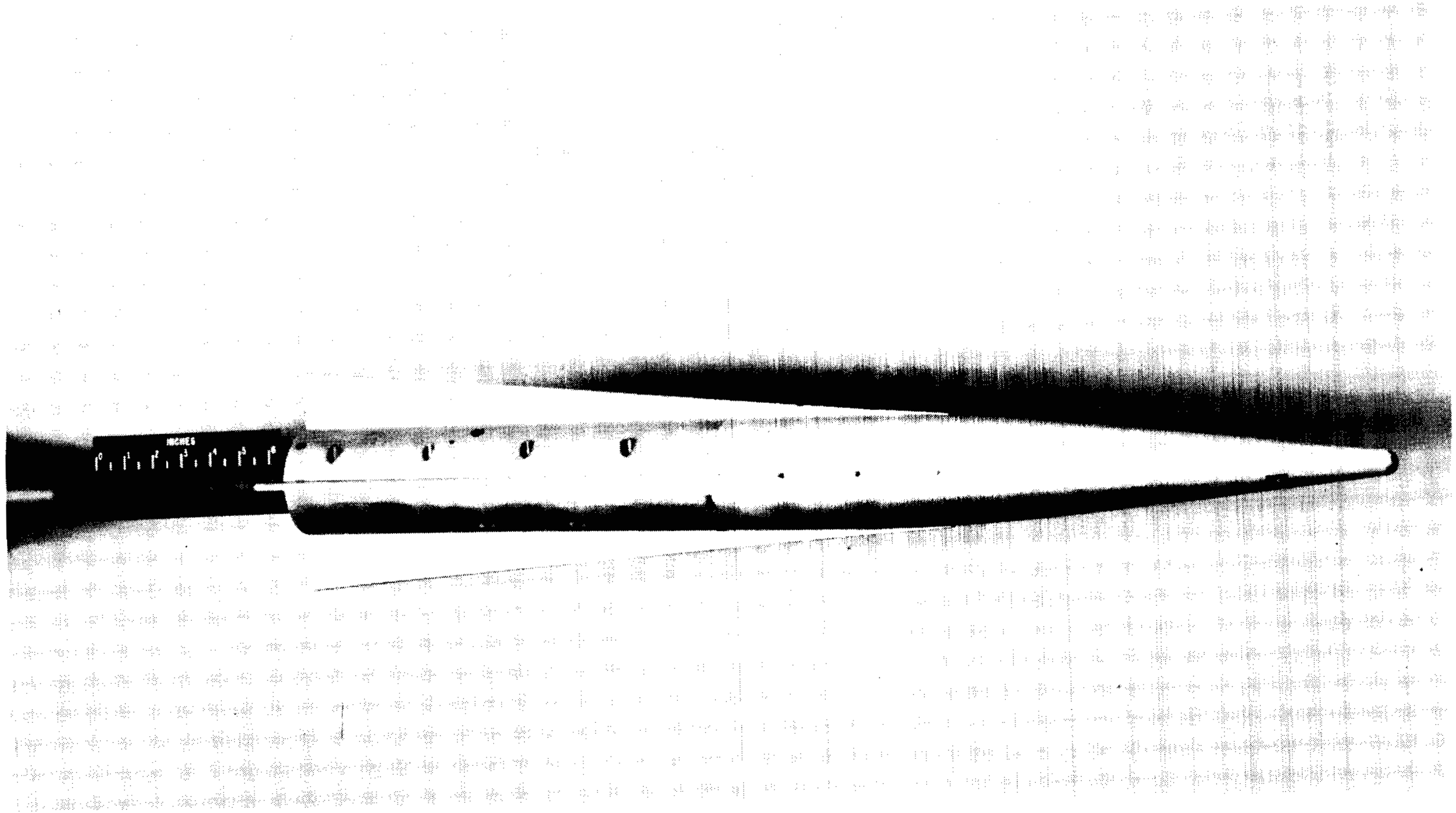

(b) Body with 5° fins. L-57-2414

Figure 4.- Concluded.

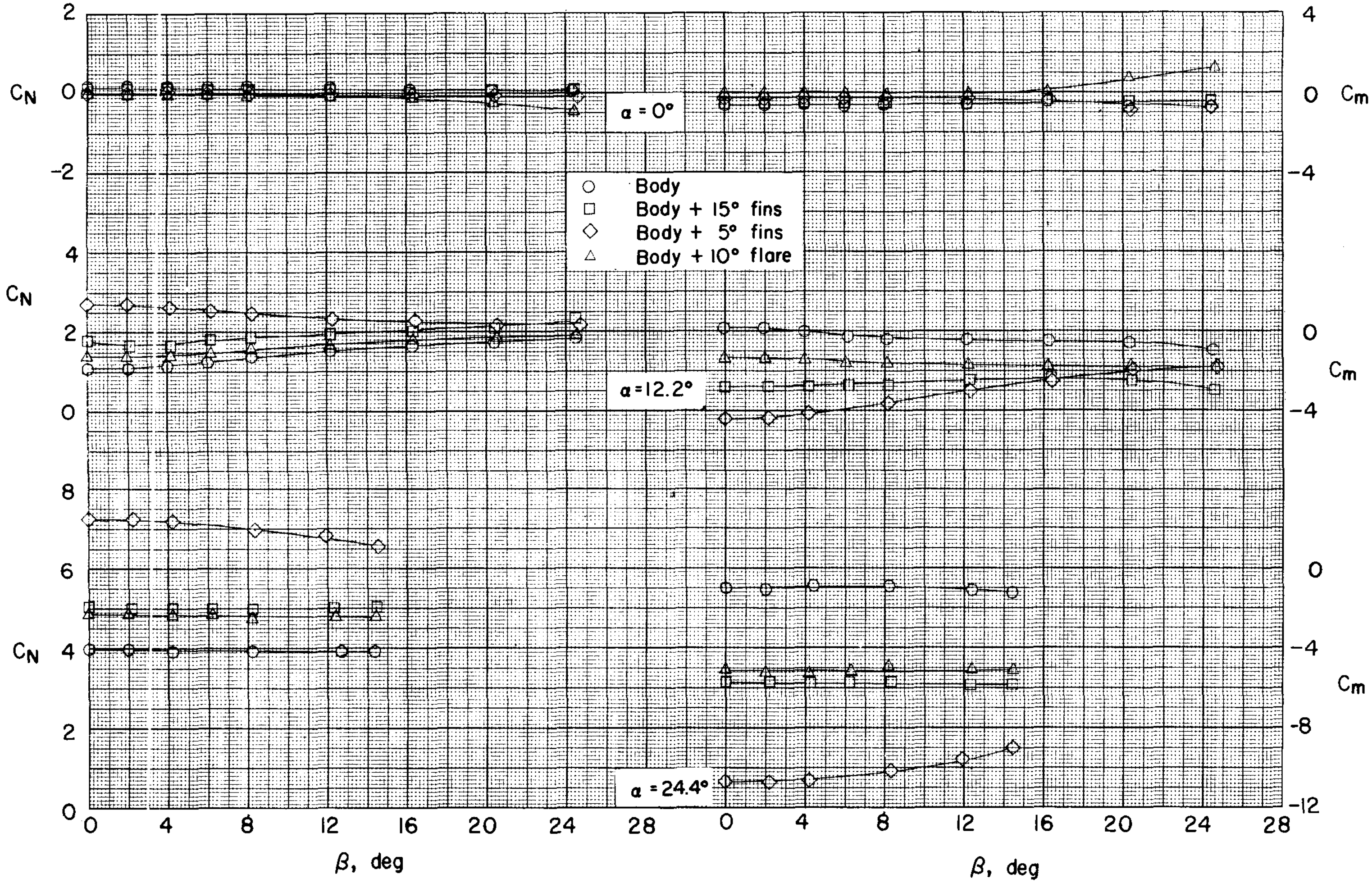

Figure 5.- Effects of fin plan form and afterbody flare on the aerodynamic characteristics of the body.

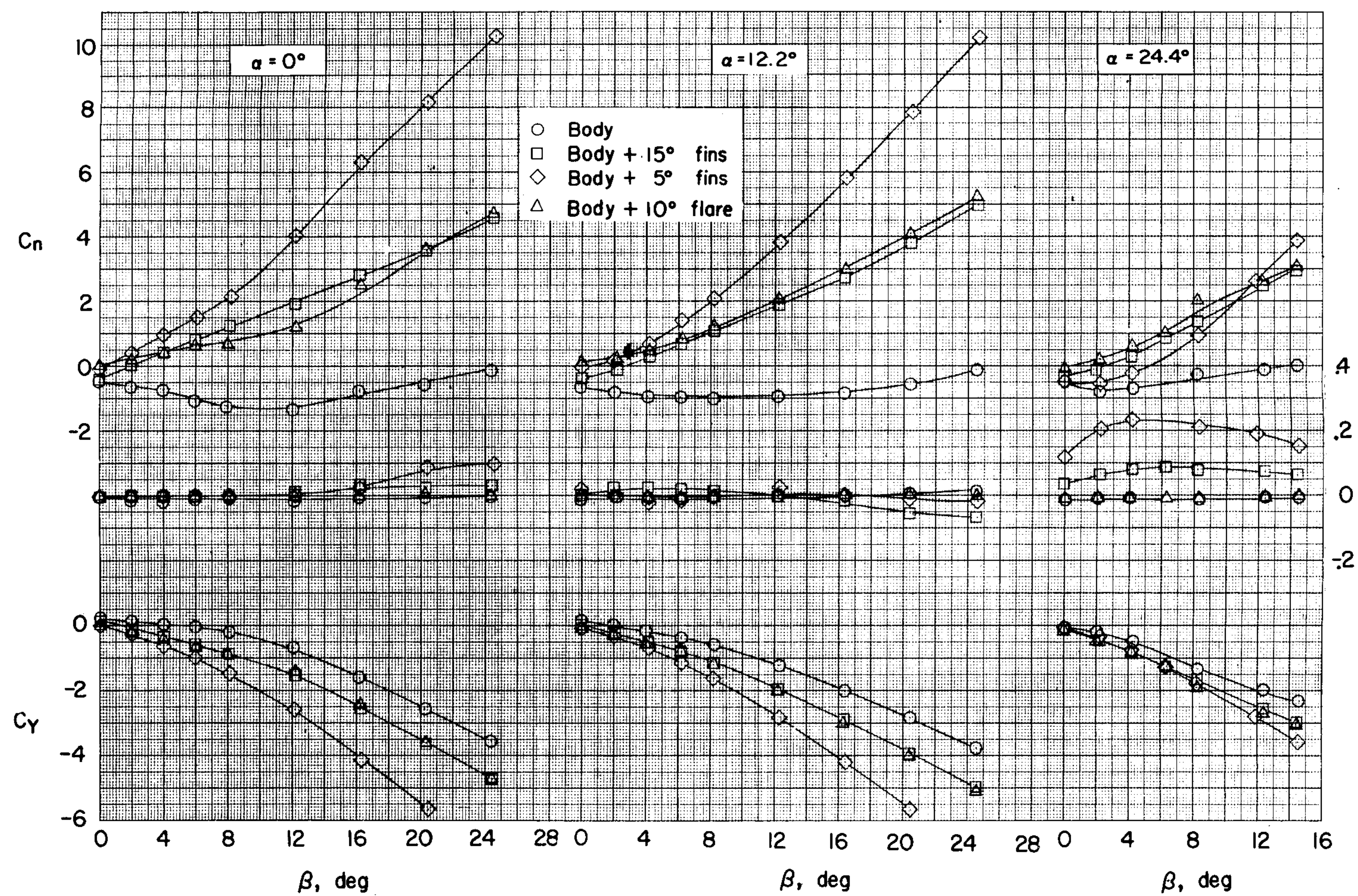

Figure 5.- Concluded.

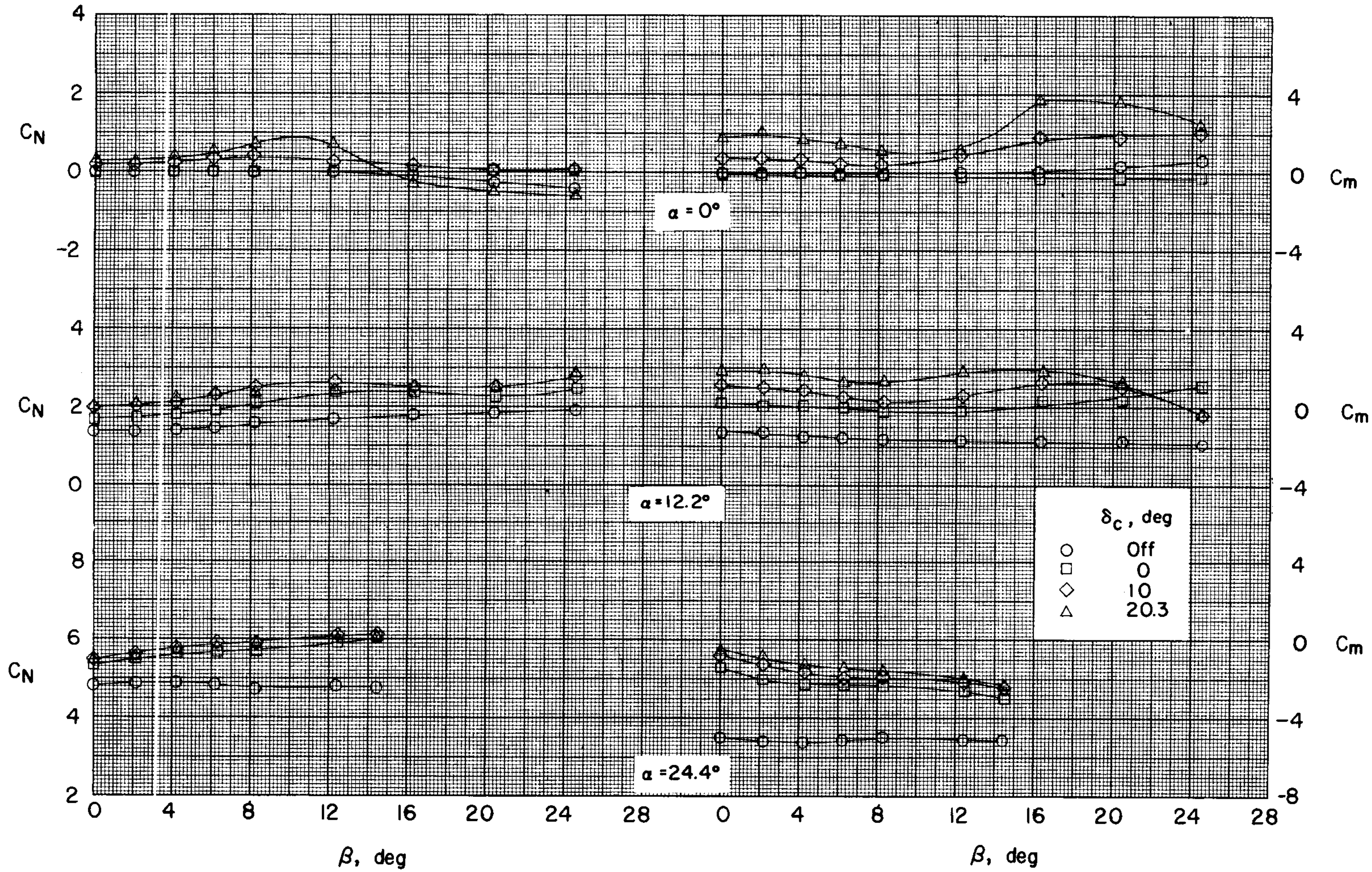

Figure 6.- Effects of canard-control deflection on the aerodynamic characteristics of the body with 10° flared afterbody and canard control C_1.

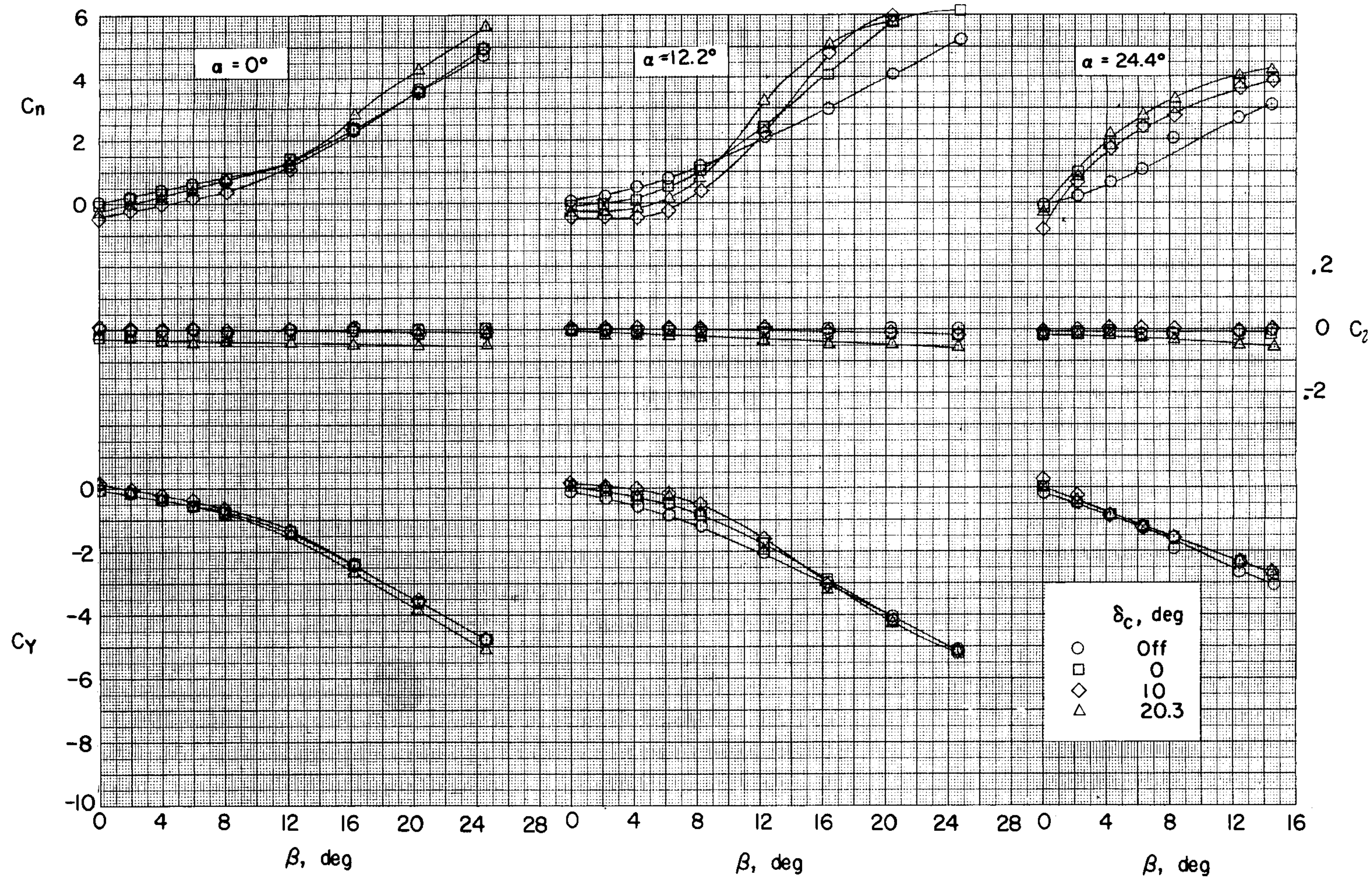

Figure 6.- Concluded.

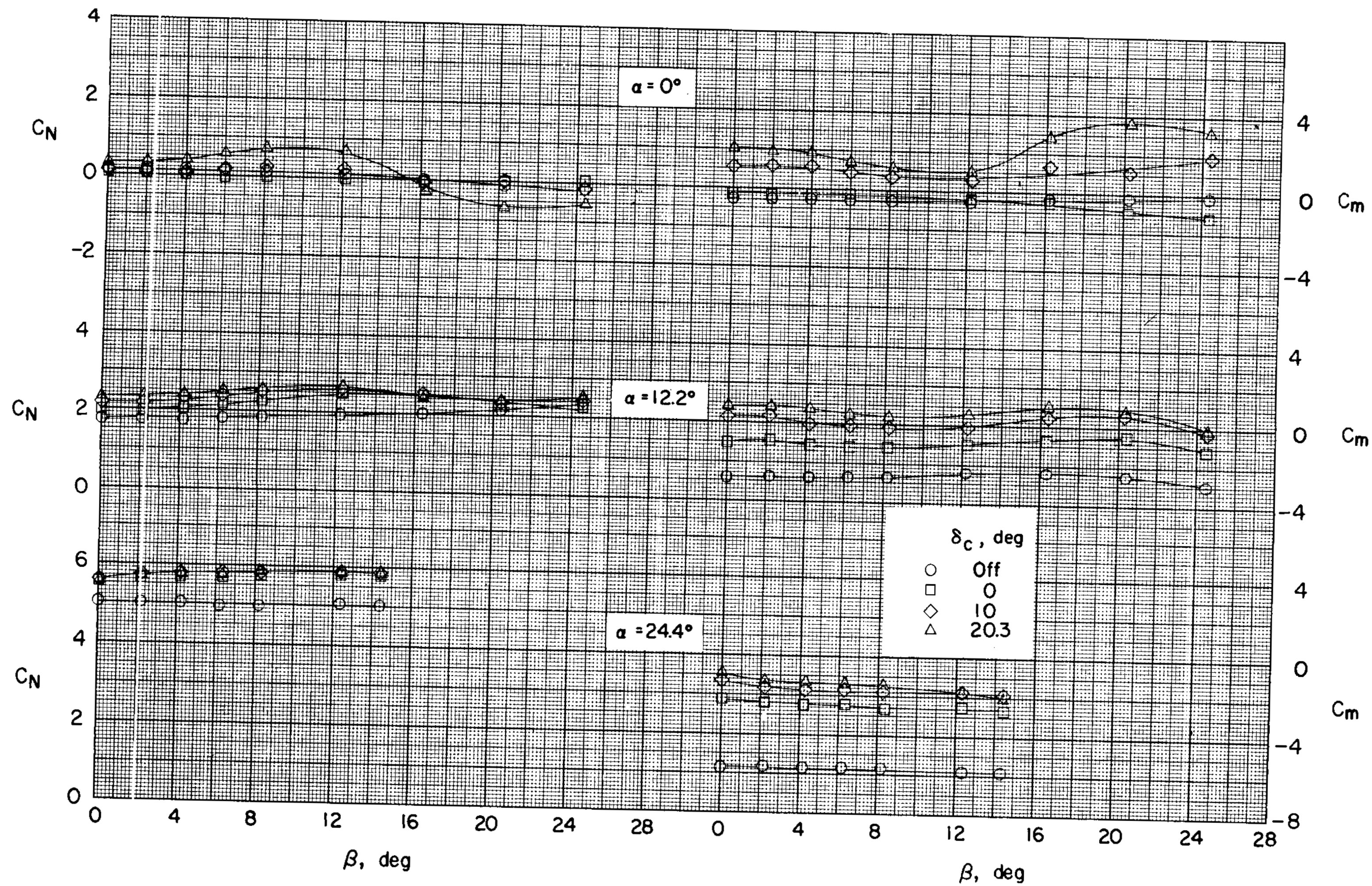

Figure 7.- Effects of canard-control deflection on the aerodynamic characteristics in sideslip of the body with 15° fins and canard control C_1.

[redacted]

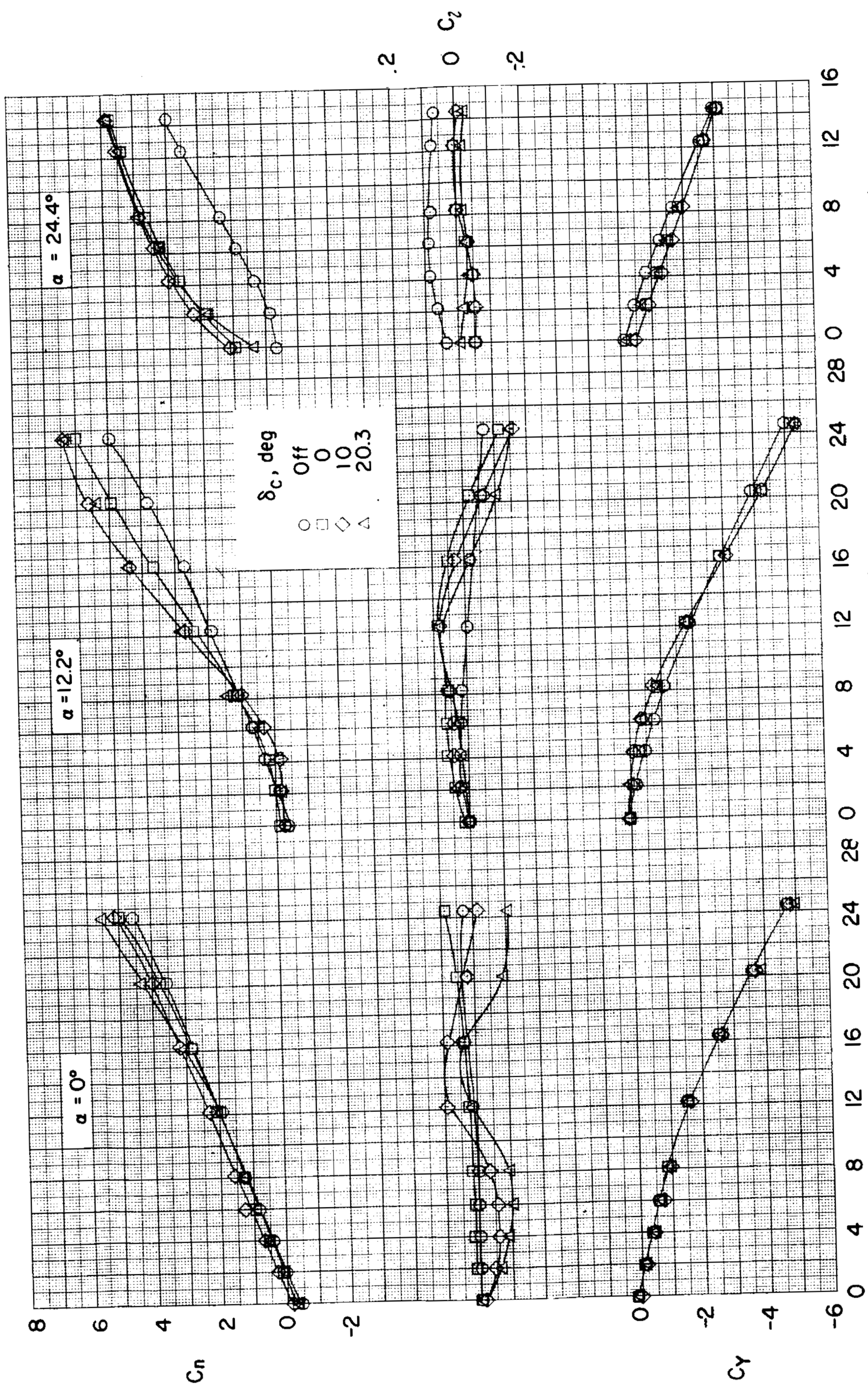

Figure 7.- Concluded.

L-262

[redacted]

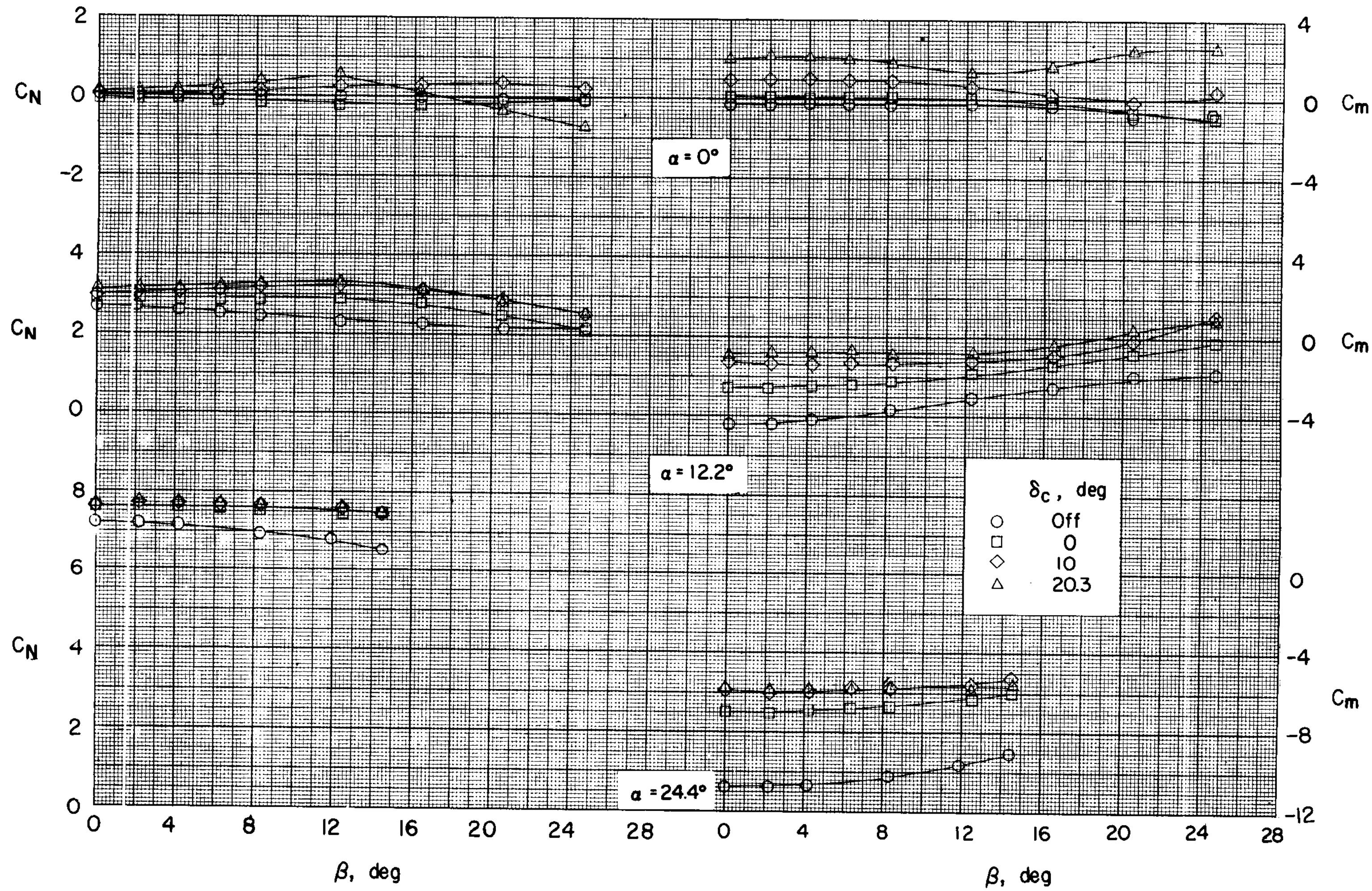

(a) Canard control C_1.

Figure 8.- Effects of canard-control deflection on the aerodynamic characteristics in sideslip of the body with 5° fins and various canard-control configurations.

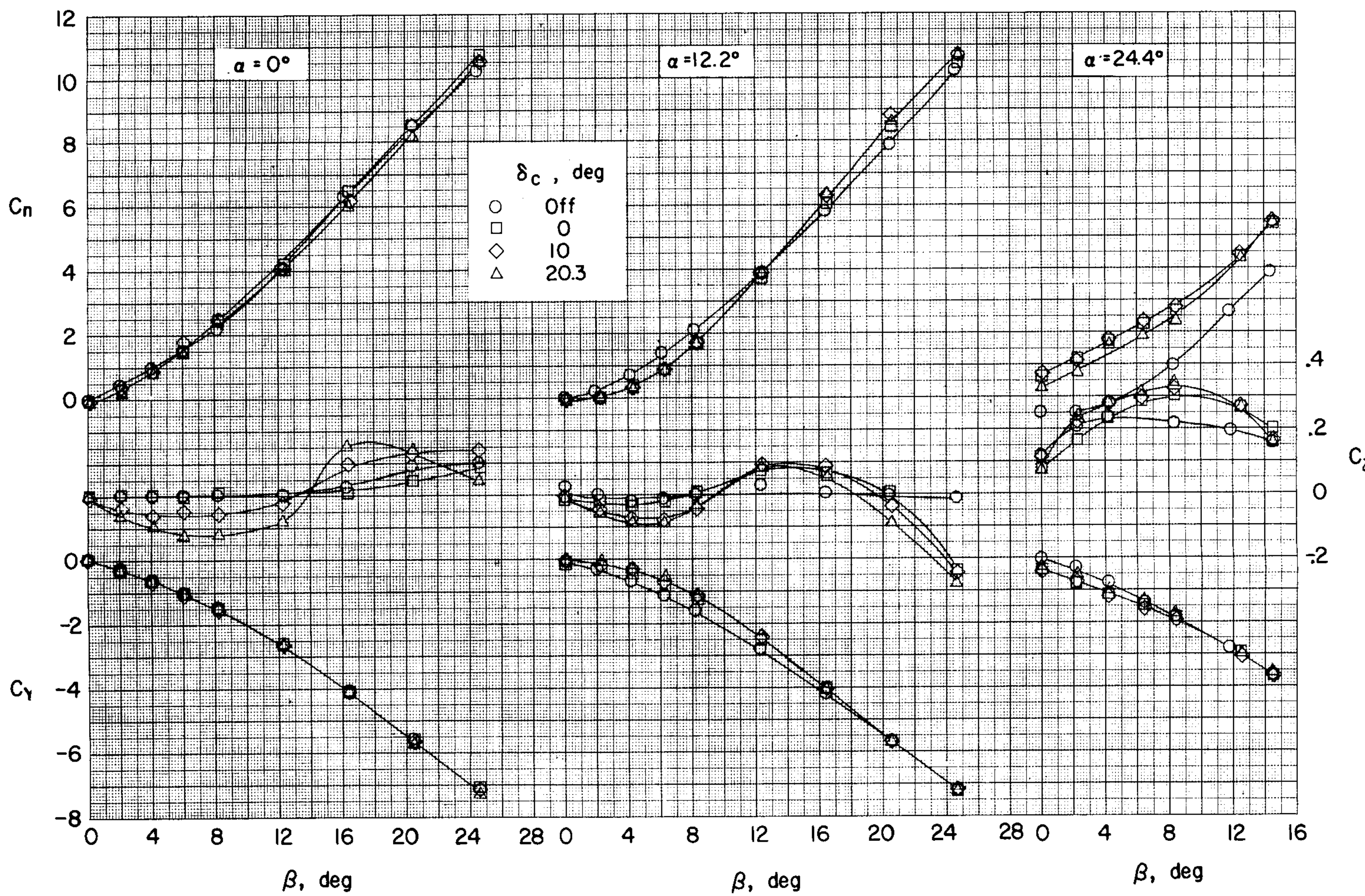

(a) Canard control C_1. Concluded.

Figure 8.- Continued.

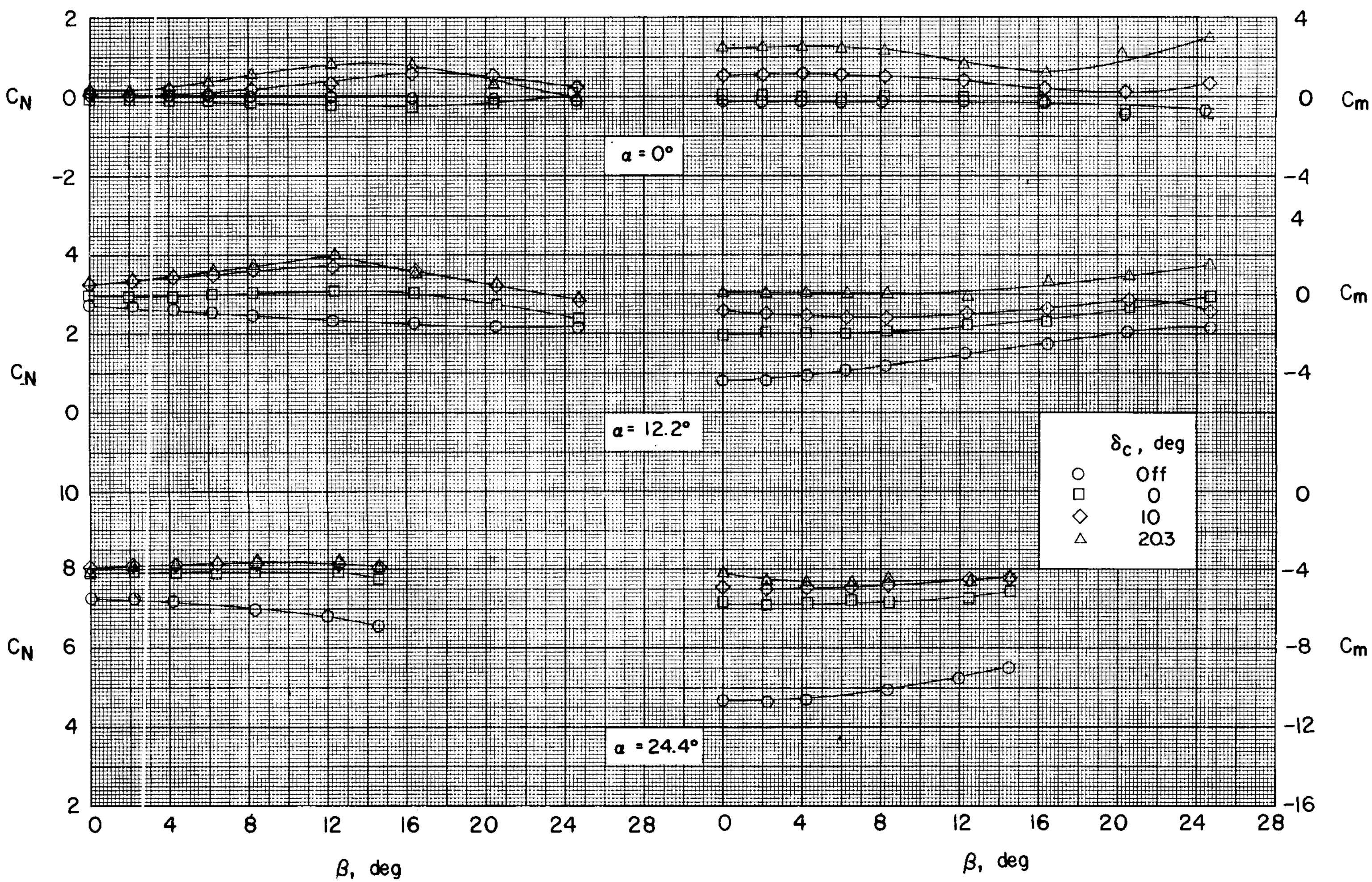

(b) Canard control C_2.

Figure 8.- Continued.

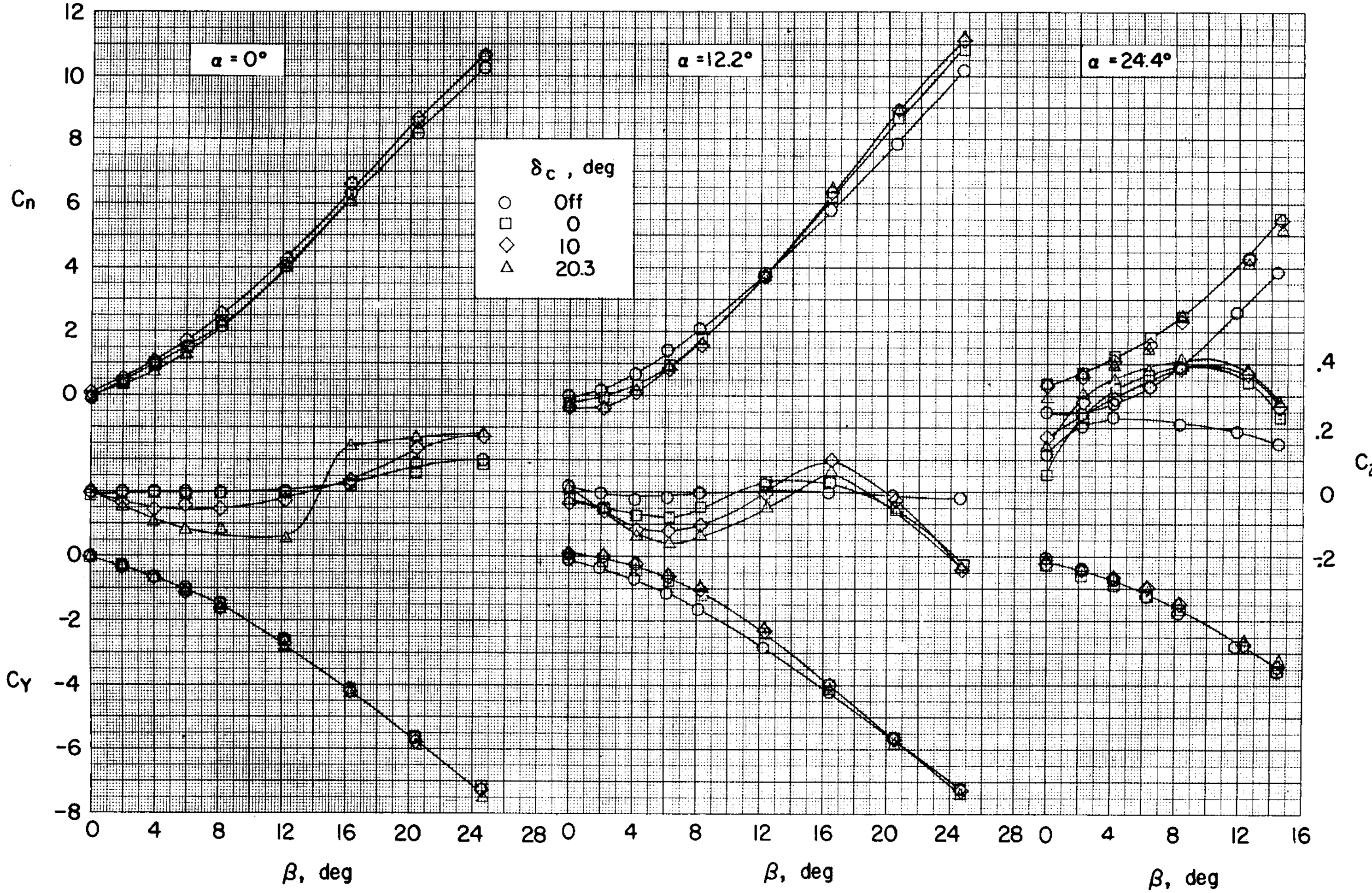

(b) Canard control C_2. Concluded.

Figure 8.- Continued.

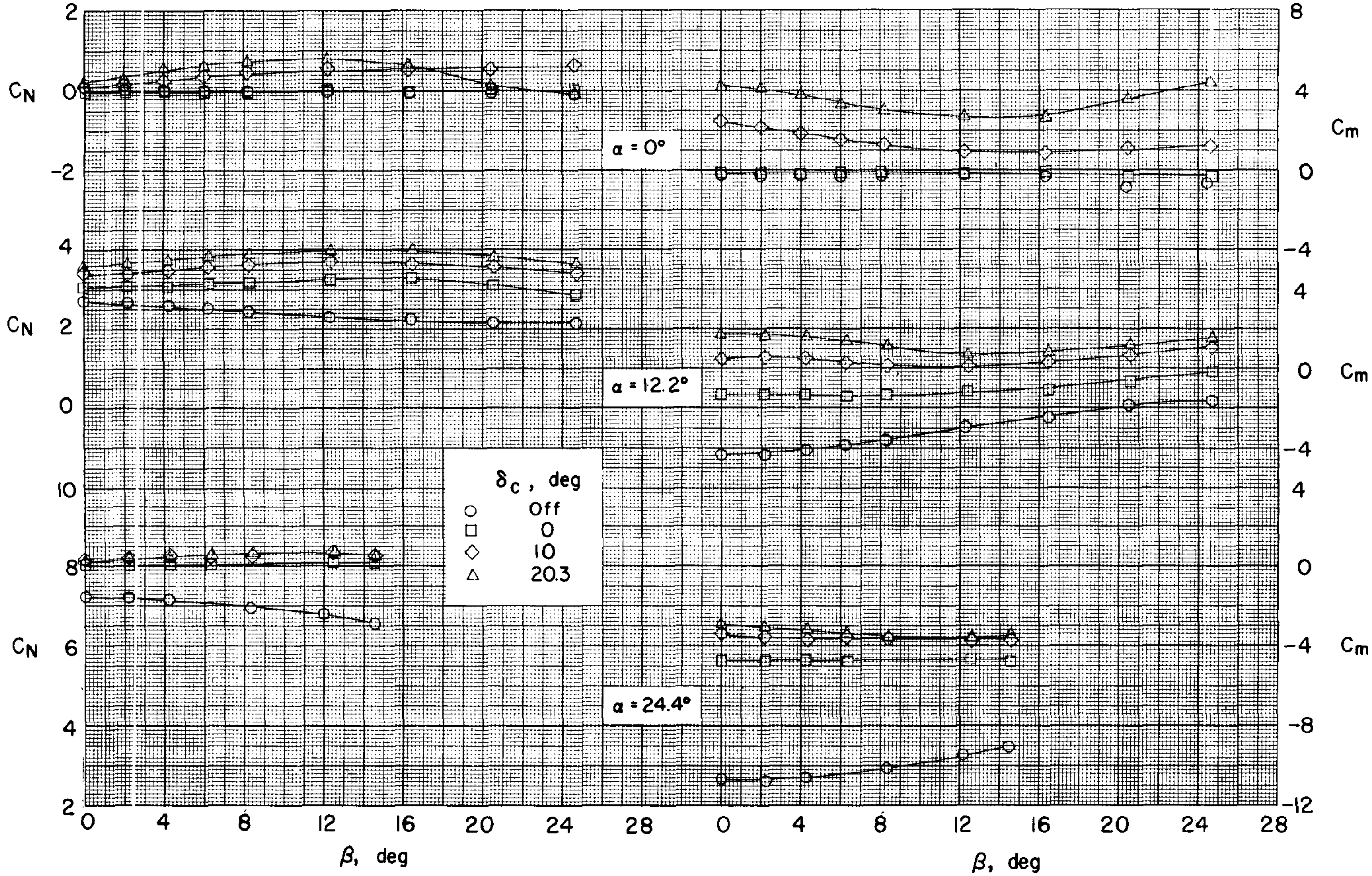

(c) Canard control C_3.

Figure 8.- Continued.

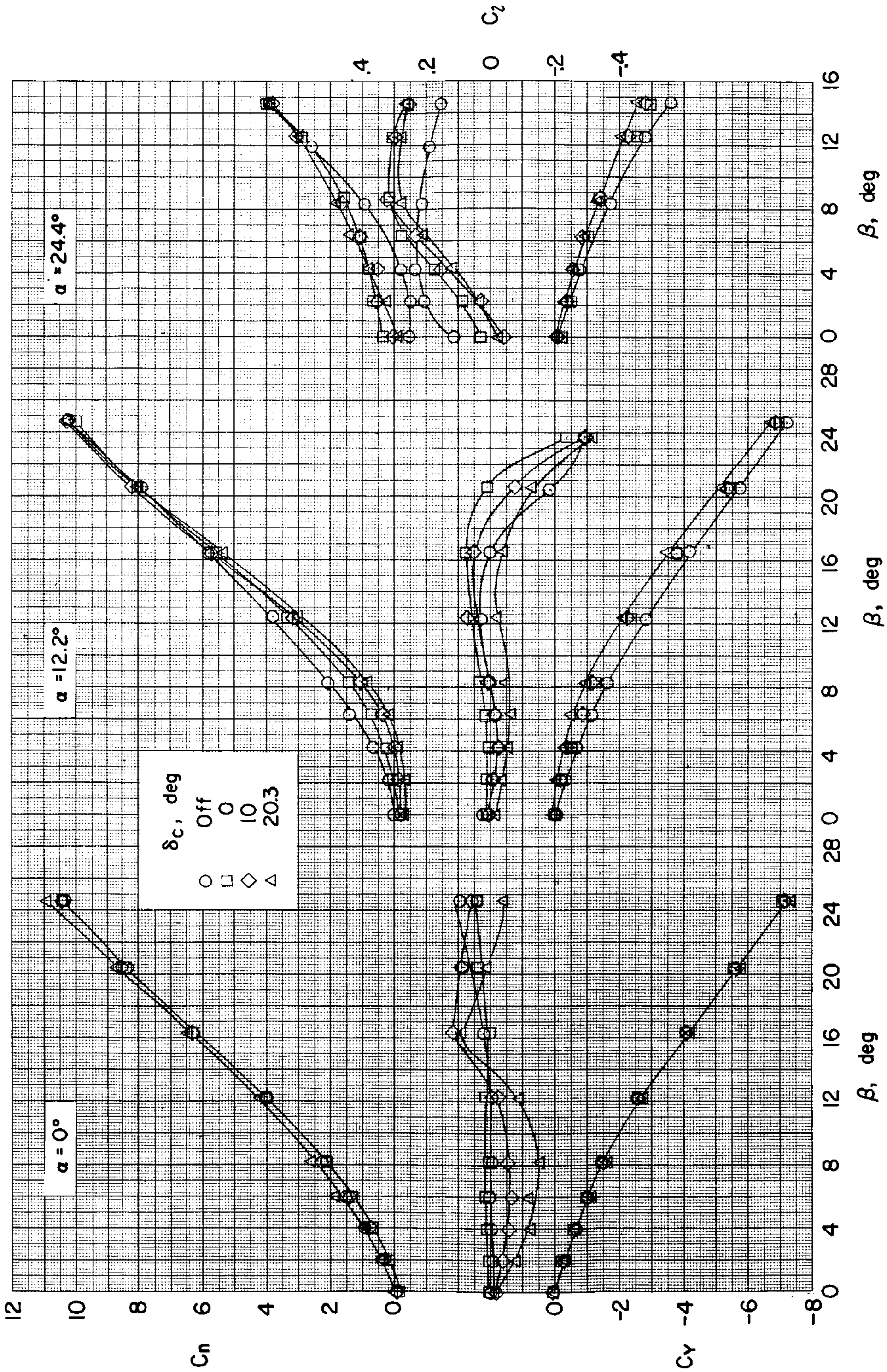

(c) Canard control C_l. Concluded.

Figure 8.- Concluded.

[redacted]